

Monte Carlo Renormalization Flows in the Space of Relevant and Irrelevant Operators: Application to Three-Dimensional Clock Models

Hui Shao^{1,2,*}, Wenan Guo^{3,2,†} and Anders W. Sandvik^{4,5,2,‡}

¹Center for Advanced Quantum Studies, Department of Physics, Beijing Normal University, Beijing 100875, China

²Beijing Computational Science Research Center, Beijing 100193, China

³Department of Physics, Beijing Normal University, Beijing 100875, China

⁴Department of Physics, Boston University, 590 Commonwealth Avenue, Boston, Massachusetts 02215, USA

⁵Beijing National Laboratory for Condensed Matter Physics and Institute of Physics, Chinese Academy of Sciences, Beijing 100190, China



(Received 5 June 2019; accepted 30 January 2020; published 27 February 2020)

We study renormalization group flows in a space of observables computed by Monte Carlo simulations. As an example, we consider three-dimensional clock models, i.e., the XY spin model perturbed by a Z_q symmetric anisotropy field. For $q = 4, 5, 6$, a scaling function with two relevant arguments describes all stages of the complex renormalization flow at the critical point and in the ordered phase, including the crossover from the $U(1)$ Nambu-Goldstone fixed point to the ultimate Z_q symmetry-breaking fixed point. We expect our method to be useful in the context of quantum-critical points with inherent dangerously irrelevant operators that cannot be tuned away microscopically but whose renormalization flows can be analyzed as we do here for the clock models.

DOI: 10.1103/PhysRevLett.124.080602

The renormalization group (RG) is a powerful framework both for conceptual understanding of phase transitions and for calculations [1–3]. A key concept is that a universal critical point can be stable or unstable in the presence of perturbations, depending on their scaling dimensions. Similarly, an ordered state can also be stable or unstable under the influence of perturbations. Under a RG process, a system flows in a space of couplings which change as the length scale is increased under coarse graining of the microscopic interactions, until finally reaching a fixed point corresponding to a phase or phase transition. At this point, all the initially present irrelevant couplings have decayed to zero.

RG flows can also be defined by physical observables obtained by Monte Carlo (MC) simulations, allowing controlled finite-size scaling analysis—sometimes referred to as phenomenological renormalization [3–6]. Here we extend the standard finite-size scaling of a single observable to an entire flow in a space of two observables associated with relevant or irrelevant couplings. The method is particularly useful for quantifying dangerously irrelevant perturbations (DIPs)—those that are irrelevant at a critical point but become relevant upon coarse graining inside an adjacent ordered phase [7].

Scaling and RG flows.—Consider a d -dimensional lattice model of length L which can be tuned to a critical point by a relevant field t , e.g., the temperature ($t = T_c - T$). With a local operator m_i and its conjugate field h , we add $h \sum_i m_i \equiv hM \equiv hL^d m$ to the Hamiltonian H . In a conventional RG calculation, a flowing field h' is

computed under a scale transformation. Here we will instead vary the system size, which effectively lowers the energy scale, and calculate the response $\langle m \rangle$ using MC simulations. Together with some quantity Q characterizing the critical point and phases of the system, we can trace out curves (MC RG flows) $(Q, \langle m \rangle)_L$ as L increases for fixed values of h and T . These flows are very similar to conventional RG flows in the space (t, h') .

The singular part of the free-energy density takes the form $f_s(t, h, L) = L^{-d} F_s(tL^{1/\nu}, hL^y)$. At $t = 0$, the leading h dependent part is $f_s \propto hL^{y-d}$, while the statistical mechanics of H gives a contribution $h \langle m \rangle \propto hL^{-\Delta}$ from the internal energy. Thus, we obtain the well-known relation $y = d - \Delta$. The perturbation is irrelevant at the critical point if $y < 0$, but, in the case of a DIP, it eventually becomes relevant as L increases in the ordered phase. It has been known for some time that this crossover is associated with a length scale $\xi' \propto t^{-\nu'}$ which may diverge faster than the correlation length $\xi \propto |t|^{-\nu}$ [8].

To take both divergent length scales properly into account, i.e., to reach the regime where $tL^{1/\nu}$ is large, we adopt the two-length scaling hypothesis [9] and write

$$f_s(t, h, L) = L^{-d} F_s(tL^{1/\nu}, tL^{1/\nu'}, hL^y, \lambda L^{-\omega}), \quad (1)$$

where we have also included a generic scaling correction with exponent $\omega > 0$. The exponents ν' and y arise from the same DIP and there is a relationship between them that has been the subject of controversy [8,10–12]. Here we will

derive the relationship from Eq. (1) and show how the entire RG flow of two observables can be explained.

Models and observables.—We study three-dimensional (3D) classical clock models on the simple cubic lattice,

$$H = -\sum_{\langle i,j \rangle} \cos(\theta_i - \theta_j) - h \sum_i \cos(q\theta_i), \quad (2)$$

with $\theta \in [0, 2\pi)$. Based on previous studies [8,10–16], for $q \geq 4$ the phase transition for fixed h at $T = T_c$ belongs to the 3D U(1) universality class, i.e., the clock field h is irrelevant. However, for $T < T_c$ it is relevant, reducing the order parameter symmetry from U(1) to Z_q when observed above the DIP length scale ξ'_q .

In our MC simulations [17], for a given spin configuration we compute $M_x = \sum_i \cos(\theta_i)$ and $M_y = \sum_i \sin(\theta_i)$. With $M = (M_x^2 + M_y^2)^{1/2}$ and $\Theta = \arccos(M_x/M)$, an angular order parameter can be defined as

$$\phi_q = \langle \cos(q\Theta) \rangle, \quad (3)$$

which becomes nonzero in response to the Z_q field. This quantity was used to study the length scale ξ'_q [10,11,13] (with a slightly different definition in Refs. [10,13]), but here we will use it in a different way. For $T \geq T_c$, $\phi_q \rightarrow 0$ when $L \rightarrow \infty$, while $\phi_q \rightarrow 1$ for $T < T_c$. We will use ϕ_q in combination with the Binder cumulant, $U = 2 - \langle M^4 \rangle / \langle M^2 \rangle^2$, which takes the limiting forms $U \rightarrow 0$ ($T > T_c$), $U \rightarrow 1$ ($T < T_c$), and $U \rightarrow U_{XY} \approx 0.757$ (at $T = T_c$ with 3D XY universality [18]).

MC RG flows.—Figure 1 shows flows of $(U, \phi_q)_L$ for the $q = 6$ “hard” model, i.e., $h \rightarrow \infty$ in Eq. (2). Results for $q = 4, 5$ are discussed in Supplemental Material (SM) [19], where we also determine $T_c(h)$ for $q = 4, 5, 6$. The RG process is manifested in the flows with increasing L of the

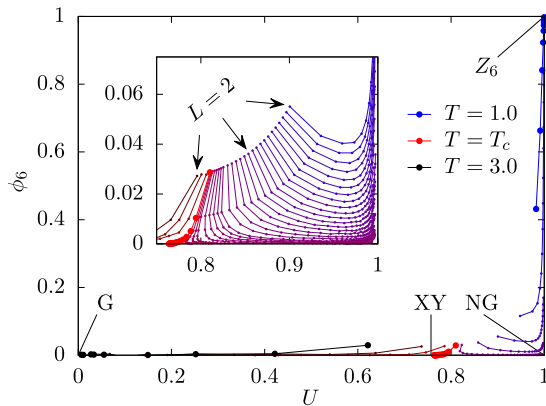


FIG. 1. MC RG flows for $q = 6$. Each set of connected dots represents a fixed T and sizes $L = 2, 3, 4, \dots$. The sets for the highest and lowest T and $T = T_c$ are shown with bigger dots in black, red, and blue, respectively. The inset shows detailed flows in the critical region.

two observables at fixed T . The high- T Gaussian fixed point (G) is at $(U, \phi_q) = (0, 0)$, the XY critical point at $(U_{XY}, 0)$, the U(1) symmetry-breaking Nambu-Goldstone (NG) point at $(1, 0)$, and the Z_q symmetry-breaking point at $(1, 1)$. For $T \geq T_c$, we observe simple flows to the fixed points, while for $T < T_c$ there are two stages in the flow away from the XY point: first toward the NG point and then a NG to Z_q crossover. While this multistage flow is expected based on previous RG results [8,11,12], our description with a phenomenological scaling function for accessible observables provides a more practical and intuitive framework for numerical simulations.

Scaling dimensions.—We first study the scaling dimension y_q of the Z_q field, following the red curve that tends to the XY fixed point in Fig. 1. Previous MC estimates used Z_q anisotropy correlators in the pure XY model for $q = 4$ [16]. Since the Z_q field is irrelevant for $q \geq 4$, the decay power $2\Delta_q$ of the correlation function is larger than 6, which makes it difficult to determine Δ_q accurately (see SM [19] for some results). The decay of the induced ϕ_q is analyzed in Fig. 2 for $q = 4, 5, 6$ at selected h values. The results listed in Table I demonstrate that ϕ_q scales as $M = L^d m$ in the general discussion above, i.e., $\phi_q \propto L^{-\Delta_q+d} = L^{-|y_q|}$.

For $q = 4$, the Z_q field may only be irrelevant for small h ; the hard model ($h = \infty$) is equivalent to two decoupled Ising models, and for $h = 2$ the transition already seems to not be in the XY universality class [13]. Here we use $h = 1$. Our simulations extend up to $L = 120$ for $q = 4$ but smaller for larger q because of the long runs needed to obtain sufficiently small error bars on ϕ_q . To reduce effects of scaling corrections we have excluded small systems until a good fit is obtained. Our result $y_4 = -0.114(2)$ agrees well with the best previous numerical result [16], but the error bar is smaller. It also matches a high-order non-perturbative expansion [12]. For $q = 5$, we have used joint

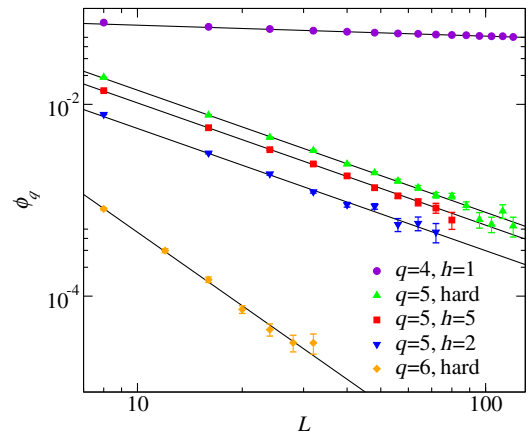


FIG. 2. Log-log plot of the critical angular order parameter ϕ_q versus the linear system size L for several q and h values. The fitting lines correspond to the power-law form $\phi_q \propto L^{-|y_q|}$ and the resulting exponents are summarized in Table I.

TABLE I. Scaling dimensions y_q of the Z_q field for $q = 4, 5, 6$. The numbers in parentheses indicate the statistical errors (1 standard deviation) of the preceding digit.

$-y_q$	q		
	4	5	6
Ref. [8]	0.2	1.5	3.0
Ref. [12]	0.114	1.16	2.29
Refs. [11,16]	0.108(6)	1.25	2.5
Ref. [20]	0.128(6)	1.265(6)	2.509(7)
This work	0.114(2)	1.27(1)	2.55(6)

fit to data for several h values, with a common exponent but different prefactors. Our result $y_5 = -1.27(1)$ is close to an extrapolated value from simulations for smaller q [11] but differs significantly from the field-theory expansions [8,12]. For $q = 6$, we obtain $y_6 = -2.55(6)$, which again agrees well with the extrapolated value [11] but differs from those in Refs. [8,12]. For all the q values studied, our results show that the first-order ϵ expansion [8] overestimates y_6 , while the nonperturbative expansion [12] underestimates it for $q > 4$. All results agree well with a very recent MC calculation of an optimized correlation function [20].

Having determined the scaling dimensions, the Z_q order parameter in the ordered phase takes the form

$$\phi_q = L^{y_q} \Phi(tL^{1/\nu}, tL^{1/\nu'_q}), \quad (4)$$

where we neglect the irrelevant arguments in Eq. (1) as they merely produce corrections here. We apply this form to curves such as those shown in Fig. 1, primarily by defining distances to the various fixed points. We study $q = 6$ specifically but keep the general- q notation.

Scaling near the XY point.—Though the critical point is well known, it is still useful to study the flows in the two-dimensional space in Fig. 1. We analyze the minimum distances of the $T < T_c$ curves to $(U_{XY}, 0)$. Here, $tL^{1/\nu'_q} \ll tL^{1/\nu} \ll 1$ in Eq. (4), and to leading order

$$\phi_q \propto L^{y_q} (1 + tL^{1/\nu}), \quad (5)$$

where we do not include unimportant factors for simplicity. The Binder cumulant scales as

$$U = U(tL^{1/\nu}) = U_{XY} + tL^{1/\nu} + L^{-\omega}, \quad (6)$$

where ω is the smallest correction exponent affecting U . The scaling form (i.e., without unimportant factors) of the distance d_1 to the XY fixed point is

$$d_1 \propto \sqrt{(tL^{1/\nu} + L^{-\omega})^2 + L^{2y_q} (1 + tL^{1/\nu})^2}. \quad (7)$$

Since $\omega \ll |y_6|$, the first term in the square root dominates; $d_1 \propto tL^{1/\nu} + L^{-\omega}$, i.e., $d_1 \rightarrow U - U_{XY}$ here (but not

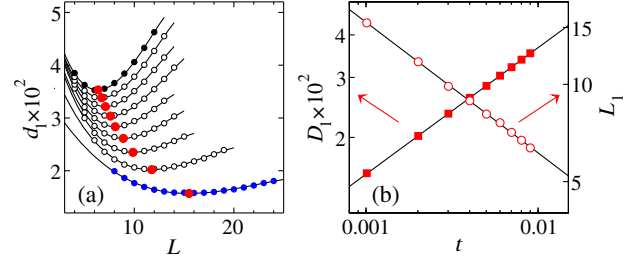


FIG. 3. (a) Distance $d_1(L)$ to the XY fixed point. Black and blue solid circles correspond to $T = 2.193$ and $T = 2.201$, respectively, and open circles show temperatures in between. The minimums (red circles) were obtained by polynomial fits. (b) Power-law behaviors in t of the minimum distance D_1 and corresponding size L_1 [red dots in (a)].

necessarily in general). Minimizing for fixed t gives the distance D_1 and the corresponding system size L_1 ,

$$\begin{aligned} D_1 &\propto t^{\omega/(1/\nu+\omega)} = t^{0.345(6)}, \\ L_1 &\propto t^{-1/(1/\nu+\omega)} = t^{-0.440(4)}, \end{aligned} \quad (8)$$

where we have used $\nu = 0.6717(1)$ and $\omega = 0.785(20)$ [18]. Figure 3(a) shows d_1 versus L and Fig. 3(b) shows power-law fits to $D_1(t)$ and $L_1(t)$, where the exponents are $0.372(1)$ and $-0.404(4)$, respectively. These values are in reasonable agreement with Eq. (8) considering scaling corrections for the rather small sizes [19] and the neglected subleading ϕ_6 contribution in Eq. (7). The error bars reflect only statistical fluctuations.

Another characteristic of the $T < T_c$ curves in Fig. 1 is the minimum distance to the horizontal axis. This RG stage between the XY and NG fixed points is still governed by the XY criticality because $tL^{1/\nu}$ and tL^{1/ν'_q} are both small. Since $tL^{1/\nu'_q} \ll tL^{1/\nu}$, ϕ_q is given by Eq. (5) and the minimum value D_2 and corresponding system size therefore scale with t as (for $q = 6$)

$$D_2 \propto t^{-y_6\nu} = t^{1.71(4)}, \quad L_2 \propto t^{-\nu} = t^{-0.6717(1)}. \quad (9)$$

The expected exponents indicated above agree reasonably well with our fits in Fig. 4, where the exponents are $1.88(2)$ and $-0.60(3)$, respectively. The deviations are again likely due to scaling corrections.

Crossover exponent ν'_q .—When $tL^{1/\nu} \gg 1$ but tL^{1/ν'_q} is arbitrary, Eq. (4) must reduce to

$$\phi_q = L^{y_q} (tL^{1/\nu})^a g(tL^{1/\nu'_q}), \quad (10)$$

where the exponent a follows from the physics of the clock model. Specifically, we can ask how ϕ_q depends on L at fixed t when the U(1) symmetry is barely broken down to Z_q , i.e., when $\phi_q \ll 1$. This is a subtle issue at the heart of the long-standing controversy regarding the symmetry

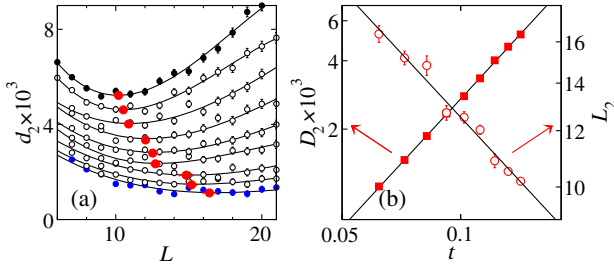


FIG. 4. (a) Distance of the curves in Fig. 1 to the x axis. The black and blue solid circles correspond to $T = 2.06$ and 2.14 , respectively, and the open circles are for equally spaced T . (b) The minimums (red dots) in (a) exhibit scaling in t of the minimum distance D_2 and the corresponding size L_2 .

crossover [8,10–12,21]. Instead of invoking physical arguments, we will here simply posit that $\phi_q \propto L^p$ in the regime where $tL^{1/\nu}$ is large but tL^{1/ν'_q} remains small [hence, $g \approx 1$ in Eq. (10)], and later show how p can be consistently determined from the MC RG flows. Thus, we have $a = \nu(p - y_q)$ in Eq. (10):

$$\phi_q = L^p t^{\nu(p-y_q)} g(tL^{1/\nu'_q}). \quad (11)$$

This form should apply also when $\phi_q \rightarrow 1$, demanding $g \rightarrow (tL^{1/\nu'_q})^b$ with $b = -\nu(p - y_q)$ and $\nu'_q = -b/p$. Then,

$$\nu'_q = \nu(1 - y_q/p) = \nu(1 + |y_q|/p), \quad (12)$$

which for $p = 3$ agrees with Ref. [10], while for $p = 2$ it agrees with Refs. [11,12]. When ϕ_q deviates from 1, $g \rightarrow (tL^{1/\nu'_q})^b [1 - k(tL^{1/\nu'_q})]$, so that for large tL^{1/ν'_q} ,

$$\phi_q \rightarrow 1 - k(tL^{1/\nu'_q}), \quad (13)$$

where the function k must be dimensionless.

The exponent ν'_q in Eq. (13) can be determined by a standard data-collapse procedure [10,11]. Here we proceed in a different way: The function $k(x)$ can be Taylor expanded around some arbitrary point x_0 where $\phi_q = y_0$; $\phi_q = y_0 + a(x - x_0)$, or $\phi_q = ax + b$ for some b . For fixed t , we consider $L = L_c$ for which $\phi_q(L_c) = e$ for some e , which gives $L_c \propto t^{-\nu'_q}$. In Fig. 5(a) we extract L_c for $e = 0.5, 0.55$, and 0.6 . Analyzing the scaling behavior with t in Fig. 5(b), we find $\nu'_6 = 1.52(4)$. Thus, Eq. (12) with $|y_6| = 2.55(6)$ is satisfied if $p = 2$, in agreement with Refs. [11,12]. From Eq. (11), the initial growth of ϕ_q with L is then $\phi_q \propto L^2$, not $\propto L^3$ [10].

Near the NG fixed point.—Finally, we consider the distance to the NG fixed point $(1,0)$, where Eq. (11) applies with $g \approx 1$ ($L \ll \xi'_q$ can be tested self-consistently [19]). U is close to 1, but should remain of the form $U(tL^{1/\nu})$ because, as we will see, L and t for a given curve in the

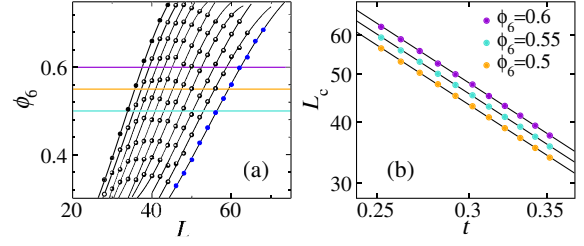


FIG. 5. (a) ϕ_6 versus L for temperatures from $T = 1.85$ (blue circles) and 1.95 (black solid circles). The crossing points with three horizontal lines at $0.5, 0.55$, and 0.6 are analyzed in (b) with a joint power law with a common exponent.

region of interest are related such that $t \rightarrow 0$ when $L \rightarrow \infty$. We need $1 - U$, which has a nontrivial scaling form,

$$1 - U \propto (tL^{1/\nu})^{-r}, \quad (14)$$

where it has been argued that, in some cases, $r = d\nu = 3\nu$ [22]. However, this result is based on subtle assumptions and may not be generic [23]. As shown in SM [19], $r = 1.52(2) \neq 3\nu$ for the XY model.

The distance to the NG fixed point is, from Eqs. (14) and (11) with $\nu(2 - y_q) = 2\nu'_q$ and $g \approx 1$,

$$d_3 = \sqrt{L^{-2r/\nu} t^{-2r} + L^4 t^{4\nu'_q}}, \quad (15)$$

and minimizing with respect to L leads to

$$D_3 \propto \sqrt{t^{2r(R-1)} + t^{4(\nu'_q - R\nu)}}, \quad L_3 \propto t^{-\nu R}, \quad (16)$$

where $R = (r + 2\nu'_q)/(r + 2\nu)$. For the $q = 6$ case we then have $D_3 \propto t^{0.9(1)}$ and $L_3 \propto t^{-1.07(3)}$. From the analysis in Fig. 6 the exponents are $1.19(3)$ and $-1.14(2)$, respectively, in reasonable agreement with the prediction, again considering that we have not included any scaling corrections. The crossover behavior around the NG point is also the most intricate of all the regions in the way the two length scales intermingle.

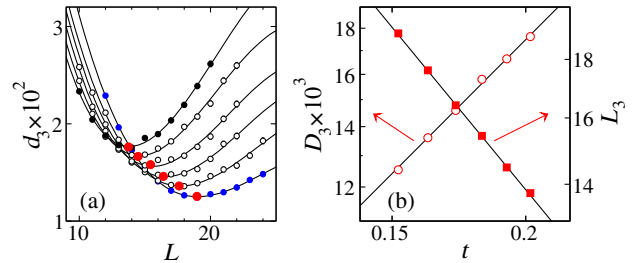


FIG. 6. (a) The distance $d_3(L)$ to the NG fixed point for temperatures between $T = 2.00$ (black solid circles) and 2.05 (blue circles) (b) Power-law behaviors in t of the minimum-distance quantities D_3 and L_3 .

Discussion.—The standard finite-size scaling hypothesis in the presence of a DIP (see, e.g., Ref. [24]) includes only $tL^{1/\nu}$ and the irrelevant field hL^y in Eq. (1), which is sufficient for extracting the critical exponents close to T_c , up to $|T - T_c| \propto L^{-1/\nu}$. As we have shown here with the clock model, the other relevant variable tL^{1/ν_q} is necessary for describing the symmetry crossover from $U(1)$ to Z_q . By considering different necessary (for scaling) limiting forms when the arguments are small or large, we have quantitatively explained the entire MC RG flows.

The controversial relationship between ν'_q and the scaling dimension y_q [8,10–12,21] involves an exponent p associated with the initial formation of an effective Z_q symmetric potential for the order parameter. Analytical RG methods for related problems, e.g., the sine-Gordon model with a weak potential, are indeed highly nontrivial and sensitive to the type of approximation used [25]. In our approach, p for a given system is obtained from numerical data and can then be used to further understanding of the subtle physics of the DIP. We have here confirmed numerically that $p = 2$ in the clock model [11,12], but this exponent is not necessarily universal—it may depend on a combination of the finite-size properties of the fixed point with the higher symmetry (here the well-understood NG point [26,27]) and the mechanisms of the DIP causing the lowering of the symmetry.

Our method should be useful in the context of deconfined quantum criticality [28–30], where a scaling ansatz with two relevant arguments was introduced to account for anomalous scaling in 2D quantum magnets [9]. There the DIP cannot be tuned away (unlike some fermionic models [31]), because it is connected to the lattice itself. Thus, the method introduced here of studying scaling and RG flows in the presence of a finite DIP is ideal.

We would like to thank Ribhu Kaul, Chengxiang Ding, Jun Takahashi, and Xintian Wu for valuable discussions. H. S. was supported by the Fundamental Research Funds for the Central Universities under Grant No. 310421119 and by the NSFC under Grant No. 11734002. W. G. was supported by NSFC under Grants No. 11734002 and No. 11775021. A. W. S. was supported by the NSF under Grant No. DMR-1710170 and by a Simons Investigator Award, and he also gratefully acknowledges support from Beijing Normal University under YingZhi Project No. C2018046. This research was supported by the Super Computing Center of Beijing Normal University and by Boston University’s Research Computing Services.

* huishao@bnu.edu.cn

† waguo@bnu.edu.cn

‡ sandvik@bu.edu

- [1] K. G. Wilson, Renormalization group and critical phenomena. I. Renormalization group and the Kadanoff scaling picture, *Phys. Rev. B* **4**, 3174 (1971).
- [2] K. G. Wilson, Renormalization group and critical phenomena. II. Phase-space cell analysis of critical behavior, *Phys. Rev. B* **4**, 3184 (1971).
- [3] M. E. Fisher and M. B. Barber, Scaling Theory for Finite-Size Effects in the Critical Region, *Phys. Rev. Lett.* **28**, 1516 (1972).
- [4] K. Binder, Critical Properties from Monte Carlo Coarse Graining and Renormalization, *Phys. Rev. Lett.* **47**, 693 (1981).
- [5] J. M. Luck, Corrections to finite-size-scaling laws and convergence of transfer-matrix methods, *Phys. Rev. B* **31**, 3069 (1985).
- [6] U. Wolff, Precision check on the triviality of the ϕ^4 theory by a new simulation method, *Phys. Rev. D* **79**, 105002 (2009).
- [7] D. J. Amit and L. Peliti, On dangerously irrelevant operators, *Ann. Phys. (N.Y.)* **140**, 207 (1982).
- [8] M. Oshikawa, Ordered phase and scaling in Z_n models and the three-state antiferromagnetic Potts model in three dimensions, *Phys. Rev. B* **61**, 3430 (2000).
- [9] H. Shao, W. Guo, and A. W. Sandvik, Quantum criticality with two length scales, *Science* **352**, 213 (2016).
- [10] J. Lou, A. W. Sandvik, and L. Balents, Emergence of $U(1)$ Symmetry in the 3D XY Model with Z_q Anisotropy, *Phys. Rev. Lett.* **99**, 207203 (2007).
- [11] T. Okubo, K. Oshikawa, H. Watanabe, and N. Kawashima, Scaling relation for dangerously irrelevant symmetry-breaking fields, *Phys. Rev. B* **91**, 174417 (2015).
- [12] F. Léonard and B. Delamotte, Critical Exponents Can Be Different on the Two Sides of a Transition: A Generic Mechanism, *Phys. Rev. Lett.* **115**, 200601 (2015).
- [13] S. Pujari, F. Alet, and K. Damle, Transitions to valence-bond solid order in a honeycomb lattice antiferromagnet, *Phys. Rev. B* **91**, 104411 (2015).
- [14] C. Ding, H. W. J. Blöte, and Y. Deng, Emergent $O(n)$ Symmetry in a series of three-dimensional Potts models, *Phys. Rev. B* **94**, 104402 (2016).
- [15] J. Hove and A. Sudbo, Criticality versus q in the $(2+1)$ -dimensional Z_q clock model, *Phys. Rev. E* **68**, 046107 (2003).
- [16] M. Hasenbusch and E. Vicari, Anisotropic perturbations in three-dimensional $O(N)$ -symmetric vector models, *Phys. Rev. B* **84**, 125136 (2011).
- [17] U. Wolff, Collective Monte Carlo Updating for Spin Systems, *Phys. Rev. Lett.* **62**, 361 (1989).
- [18] M. Campostrini, M. Hasenbusch, A. Pelissetto, and E. Vicari, Theoretical estimates of the critical exponents of the superfluid transition in ^4He by lattice methods, *Phys. Rev. B* **74**, 144506 (2006).
- [19] See Supplemental Material at <http://link.aps.org/supplemental/10.1103/PhysRevLett.124.080602> for T_c determinations, MC flow diagrams for $q = 4, 5$, results for Z_q correlations, and the asymptotic scaling of $1 - U$.
- [20] D. Banerjee, S. Chandrasekharan, and D. Orlando, Conformal Dimensions via Large Charge Expansion, *Phys. Rev. Lett.* **120**, 061603 (2018).

- [21] Y. Ueno and K. Mitsuho, Incompletely ordered phase in the three-dimensional six-state clock model: Evidence for an absence of ordered phases of XY character, *Phys. Rev. B* **43**, 8654 (1991).
- [22] V. Privman, Finite-size scaling of critical cumulants near the ferromagnetic phase boundary, *Physica (Amsterdam)* **129A**, 220 (1984).
- [23] V. Privman, in *Finite-Size Scaling and Numerical Simulation of Statistical Systems*, edited by V. Privman (World Scientific, Singapore, 1990).
- [24] R. Kenna and B. Berche, A new critical exponent “koppa” and its logarithmic counterpart, *Condens. Matter Phys.* **16**, 23601 (2013).
- [25] I. Nándori, U.D. Jentschura, K. Sailer, and G. Soff, Renormalization-group analysis of the generalized sine-Gordon model and of the Coulomb gas for $d > \sim 3$ dimensions, *Phys. Rev. D* **69**, 025004 (2004).
- [26] P. Hasenfratz and H. Leutwyler, Goldstone boson related finite size effects in field theory and critical phenomena with $O(N)$ symmetry, *Nucl. Phys.* **B343**, 241 (1990).
- [27] I. Dimitrović, P. Hasenfratz, J. Nager, and F. Niedermayer, Finite-size effects, Goldstone bosons and critical exponents in the $d = 3$ Heisenberg model, *Nucl. Phys.* **B350**, 893 (1991).
- [28] T. Senthil, A. Vishwanath, L. Balents, S. Sachdev, and M. P. A. Fisher, Deconfined quantum critical points, *Science* **303**, 1490 (2004).
- [29] A. W. Sandvik, Evidence for Deconfined Quantum Criticality in a Two-Dimensional Heisenberg Model with Four-Spin Interactions, *Phys. Rev. Lett.* **98**, 227202 (2007).
- [30] J. Lou, A. W. Sandvik, and N. Kawashima, Antiferromagnetic to valence-bond-solid transitions in two-dimensional $SU(N)$ Heisenberg models with multispin interactions, *Phys. Rev. B* **80**, 180414(R) (2009).
- [31] Y. Liu, Z. Wang, T. Sato, M. Hohenadler, C. Wang, W. Guo, and F. F. Assaad, Superconductivity from the condensation of topological defects in a quantum spin-Hall insulator, *Nat. Commun.* **10**, 2658 (2019).